LYING POSTURE DETECTION FOR UNCONSTRAINED MEASUREMENT OF RESPIRATION AND HEARTBEAT ON A BED

Toshiharu Mukai, Kazuya Matsuo
RIKEN RTC
2271-130, Anagahora, Shimoshidami, Moriyama-ku,
Nagoya, Aichi 463-0003, Japan
email: {tosh,matsuo}@nagoya.riken.jp

Yo Kato, Atsuki Shimizu and Shijie Guo
SR Laboratory, Tokai Rubber Industries
1, Higashi 3-chome
Komaki, Aichi, City, 485-8550, Japan
email: {yoh.katoh,atsuki.shimizu,shiketsu.kaku}@tri.tokai.co.jp

ABSTRACT
Daily monitoring of respiration and heartbeat while sleeping provides basic data for the assessment of personal health and early detection of diseases. The monitoring should not interfere with natural sleep, and it is desirable that the sensor be imperceptible to the person being measured. We propose a method for non-invasive and unconstrained measurement of the lying posture, respiration and heartbeat of a person on a rubber-based tactile sensor sheet. The tactile sensor is soft, flexible, and thin, and is not uncomfortable for the person lying on it. To extract faint heartbeat signals from pressure changes detected by the sensor, precision measurement based on improvement of the S/N ratio by averaging oversampled data is needed. This process takes some time and can be performed at only a limited number of locations on the sensor. To determine the locations, we detect the lying location and posture of the measured person on the sensor by using pattern recognition based on machine learning. In this paper, we describe the measurement method and report the experimental results.

KEY WORDS
Respiration, Heartbeat, Lying Posture, Tactile Sensor, Sleep Monitoring System, AdaBoost.

1 Introduction

Monitoring of respiration and heartbeat while sleeping gives basic and important information for the assessment of personal health and early detection of diseases. For use in daily life, the monitoring should be non-invasive and unconstrained, and use of the measurement apparatus should be simple and easy.

Many methods for unconstrained measurement of respiration and/or heartbeat have been presented in the literature. In [1, 2, 3], pressure or vibration sensors in air-sealed cushions under a mattress are used to detect respiration and heartbeat. Other methods include using flexible piezoelectric film sensors [4], load cells [5], ultrasound transmitter and receiver pairs [6], and microwave Doppler radar [7]. These methods do not obtain pressure distribution patterns and cannot distinguish the lying posture of the person on a bed. When two or more persons, or a person with a pet, are on a bed, their pressure changes mix and cannot be measured separately. The information of a lying posture is also useful for deciding the sleeping condition and diagnosing problems such as sleep apnea syndrome (SAS) and decubiti. In one study, pressure distribution and respiration were measured by many pressure sensors attached on a bed [8], but heartbeat was not detected. Each method has individual problems: air-sealed cushions are several centimeters thick and so are not sufficiently thin, piezoelectric film sensors must be placed near the heart of the measured person, and other devices are relatively expensive and setting them is not easy.

We are developing a method of measuring the posture, the respiration rate, and the heart rate of a lying person by using a tactile sensor. The tactile sensor is soft, flexible, and thin, and is not uncomfortable for the lying person on it. Respiration and heartbeat obtained by the tactile sensor are extracted from pressure changes over time. These signals are small compared with the load of the person's weight. In particular, heartbeat signals are faint. To measure them, we improve their signal-to-noise (S/N) ratio by averaging oversampled data. However, the averaging process takes time and can be performed only at a limited number of locations on the tactile sensor. The suitable locations for heartbeat measurement depend on not only the lying location on the sensor but also the lying posture of the measured person. Therefore, location and posture must be detected first. In our method, we use a pattern-recognition technique based on machine learning for this purpose.

In this paper, we first explain our proposal for the lying posture, respiration rate, and heart rate measurement system. We use a rubber-based flexible tactile sensor in this system, and so we particularly describe this sensor. Next we mention how to detect respiration and heartbeat. We explain that the measurement of heartbeat must be performed at suitable locations determined by the measured person's lying location and posture. Then we describe the method to determine them by using a pattern-recognition technique based on machine learning. We describe our evaluation of this system using real data, then conclude this paper.

DOI: 10.2316/J.2014.216.818-0014

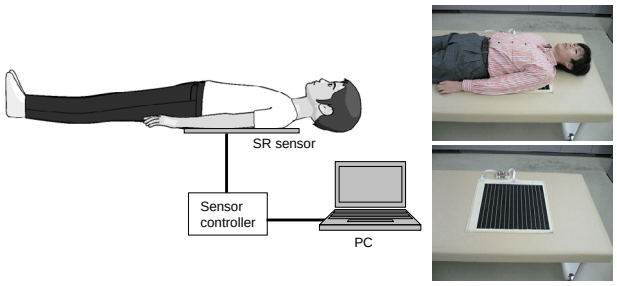

(a) (b)

Figure 1. Setup of our sleep monitoring system (a), and photos of the SR sensor with and without a person on it (b).

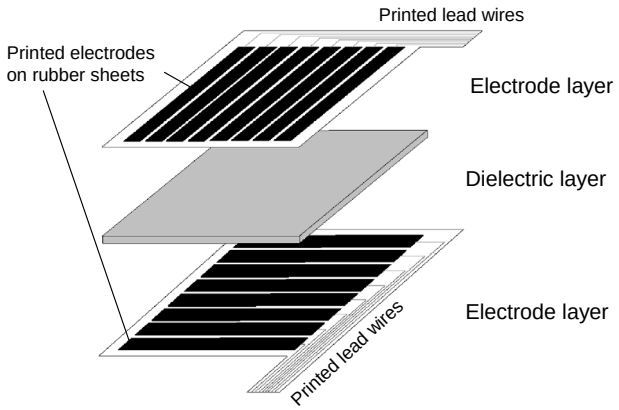

Figure 2. Schematic structure of the SR sensor.

2 Setup of the Measurement System

The setup of the lying posture, respiration, and heartbeat measurement system is shown in Figure 1 (a). The measured person lies on a tactile sensor. It is an unconstrained measurement system because the person can take a favorite lying location and posture as long as he/she is on the sensor. We developed an *SR (Smart Rubber) sensor* [9] as the tactile sensor.

The SR sensor is a rubber-based capacitive tactile sensor. It has a structure consisting of two rubber sheets with a thin dielectric layer put between them, as shown in Figure 2. Carbon-filled conductive rubber is printed on the rubber sheets to form electrodes. The electrodes on the upper and lower sheets cross orthogonally, and each crossing part becomes a capacitor, which we refer to as a *cell*. All the cells in the two-dimensional array constitute the tactile sensor.

When pressure is applied on the SR sensor, the dielectric layer deforms and the distance between the upper and lower electrodes becomes shorter. As a result, the capacitance of the cell increases. By scanning the capacitances of the cells in the SR sensor, we can detect the two-dimensional pressure distribution on the sensor. Tactile sensors based on this principle were proposed years ago, and sensor sheets that employ metal electrodes are commercially available [10], but the high cost and/or the lack of flexibility are issues for their use in healthcare situations. We developed a soft and flexible SR sensor consisting of rubber parts that include the electrodes. The electrodes are made by printing, which keeps the fabrication cost low.

Because the SR sensor is soft and flexible, it is not uncomfortable for the person lying on it. The current sensor has 16×16 cells and the pressure-sensitive area is 478 mm$\times$478 mm and 3.5 mm thick. A larger bed-size sensor is desirable and, in principle, can be made, but currently we use this size of sensor because of its availability. Photos are shown in Figure 1 (b).

The SR sensor is connected to a controller, which obtains the pressure distribution by scanning. Measuring one cell takes 184 μs, which means 47 ms for the whole sensor sheet. The pressure distribution is sent to a PC, where the lying posture, the respiration rate, and the heart rate are detected by pattern recognition and signal processing.

3 Measurement Method

The basic flow of the proposed method is shown in Figure 3. Of the cells responding to the weight of the measured person lying on the sensor, ones that are suitable for respiration and heartbeat measurement are selected. From the time series of pressure obtained from these cells, respiration and heartbeat signals are extracted by signal processing. When a person lies quietly on a bed, respiration has a frequency range of approximately 0.1–0.5 Hz, and the heartbeat has a frequency of approximately 0.9–1.5 Hz; thus, they can be extracted by, for example, bandpass filters. When only frequencies are required, we can obtain them by finding the peaks in the bandwidths. We already confirmed that respiration and heartbeat frequencies detected by this method agree with those obtained by commercial measurement apparatus [11], which used a respiration sensor with a band measuring the breast circumference and a heartbeat sensor recording the electrocardiogram (ECG).

Generally, in tactile sensors that measure pressure distribution, high-precision devices cannot be adopted for each element constituting the two-dimensional array because of cost and size limitations. Consequently, the S/N ratio of the pressure detected by tactile sensors is not high. Our SR sensor also has this problem, but the detection of respiration is still possible. For detecting heartbeat signals, which have smaller changes in pressure compared to respiration, however, we need to suppress noise and perform highly precise measurements. We improve the S/N ratio by sampling the pressure at a rate much faster than the signal frequency (oversampling) and averaging the results. As is well known, by averaging N-sampled data, the noise amplitude becomes $1/\sqrt{N}$, if the noise is random. The noise

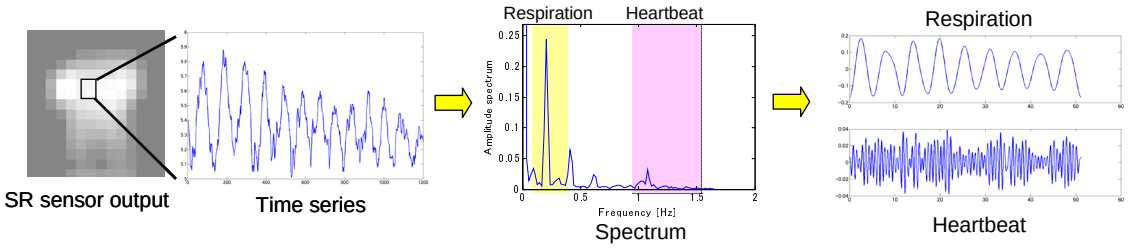

Figure 3. Extraction of respiration and heartbeat signals from SR sensor output.

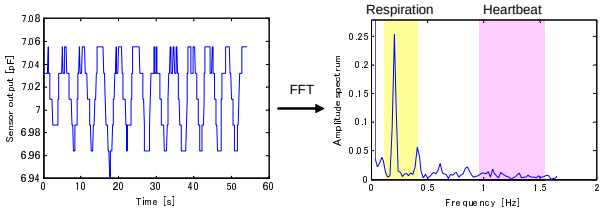

Figure 4. Time series of SR sensor output and its FFT result.

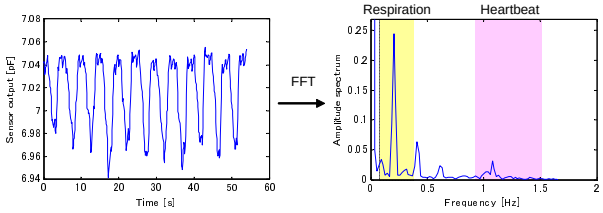

Figure 5. Time series of 36-times oversampled averaged SR sensor output and its FFT result.

can be a mix of discretization noise, thermal noise, the influence of parasitic capacitance, and so on, but here we do not further pursue the details.

Figure 4 shows a time series of the pressure detected by an SR sensor cell at a location near the heart and its fast Fourier transform (FFT) result for a person lying on the sensor in the supine posture. As the sensor output, we adopted the capacitance of the cell before it is converted to pressure. We can easily find the respiration component, which is the large oscillation. Fluctuations caused by the heartbeat are imposed on this signal, but they are small and inarticulate. In the FFT result, the peak in the respiration bandwidth is distinctive, but a clear peak cannot be found in the heartbeat bandwidth. For comparison, we show the 36-times oversampled averaged signal and its FFT result in Figure 5, where the measurement was made simultaneously with that in Figure 4. The measurement accuracy was much improved, and we could find changes possibly caused by the heartbeat. Actually, we found a distinctive peak in the heartbeat bandwidth in the FFT result.

By averaging oversampled signals in this way, we can attain the S/N ratio needed for heartbeat measurement. However, if we apply this method to all the cells in the SR sensor, too long a time is needed to realize the sampling frequency for respiration and heartbeat measurements. Thus, we confine the precision measurement to a limited number of cells. We refer to the cells as *precision cells*. We adopt 36-times oversampled averaging, used in Figure 5, for heartbeat detection. Then, using the current 16×16 SR sensor of 184 μs sampling time for one measurement, it is possible to measure the whole pressure distribution at 10 Hz, while simultaneously performing the precision measurement in 4 cells at 20 Hz. Because the number of precision cells is limited, we must set them at locations suitable for heartbeat detection.

To determine suitable locations for heartbeat measurement, we performed precision measurements at all the cells responding to the weight of the measured person. When we perform a 1024-point Fourier transform that provides a sufficient frequency resolution, the necessary measurement time is more than 51 s for one cell. In the current system, only 4 precision cells can be set at the same time; thus, we must shift their locations and perform the measurements repeatedly. When half of the cells are responding to the weight, a 16×16 SR sensor requires an approximately 30-min measurement time in total. We conducted this precision cell measurement for supine, prone, right lateral, and left lateral postures. During that time, the measured person kept the lying posture as steadily as possible. We performed the FFT on each measured cell. As an example, the obtained spectra of the pressure for a prone posture are shown in Figure 6. This illustrates that cells at limited locations can detect pressure changes caused by the heartbeat. Figure 7 shows the suitable locations for heartbeat detection determined by this method. Different measurement locations are selected for each lying posture. That is, we must detect not only the lying location but also the lying posture in order to set precision cells at locations suitable for heartbeat detection.

4 Pattern Recognition for Classifying Lying Postures

To set precision cells to suitable locations for heartbeat detection, we detect the location and posture of a person lying

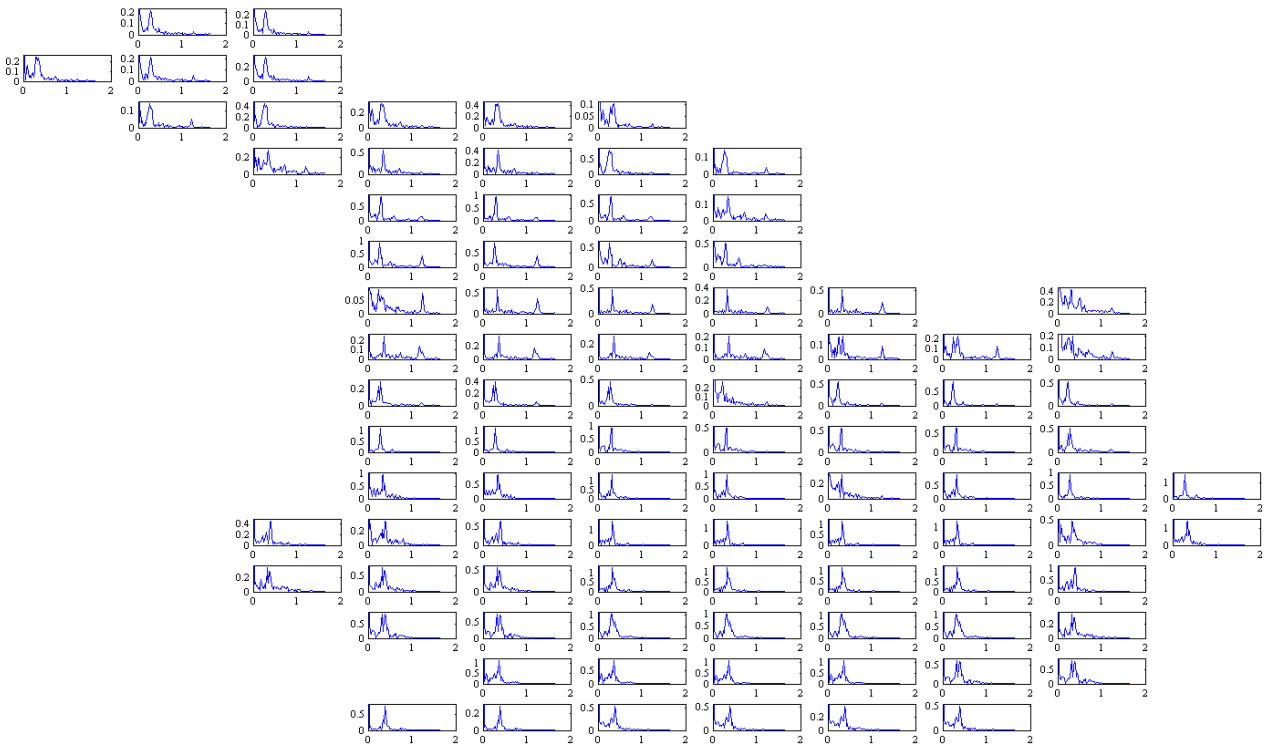

Figure 6. Spectra of pressure from different cells when a person in prone posture was on the sensor. Cells without pressure are omitted.

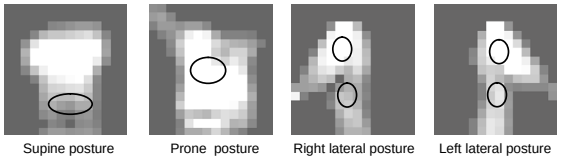

Figure 7. Suitable locations for heartbeat detection. The circles show suitable precision cell locations for different lying postures.

on the tactile sensor on the basis of the pressure pattern. Referring to human detection methods in image processing, we propose a method using machine learning. Its basic flow is shown in Figure 8. In this method, a pressure pattern is referred to as a *tactile image*.

First, we obtain sample tactile images of supine, prone, right lateral, and left lateral postures that we intend to classify. To acquire generalization ability, it is desirable that images are obtained from many people. Because of the different physiques of measured persons, the size of the figures and the pressure ranges in the tactile images are different. Furthermore, even in images from the same person, the locations and orientations of the figure in the image frame are different for each measurement trial. For efficient machine learning for constructing a classifier, we perform pre-processing to absorb these differences. Specifically, we obtain normalized images having figures with a standardized location, orientation, size, and pressure range by applying scale-change, rotation, cutting-out, and vector-normalization to the raw original images.

We construct a classifier of lying postures for the normalized tactile images obtained above by machine learning. Many methods have been proposed for machine learning, for example, support vector machines [12], neural networks [13], and random forests [14]. In our method, we adopt AdaBoost [15], which is often used in image processing. The standard AdaBoost is for two-class classification; thus, we use SAMME [16], which is an extension of AdaBoost for multi-class classification.

In SAMME, the final classifier is constructed by combining weak classifiers that generally have insufficient ability for classification. Suppose that the input as a normalized tactile image converted to a vector is $\boldsymbol{x}$, the label indicating a class to be classified is $k \in \{1, \ldots, K\}$, weak classifiers are $h_m(\boldsymbol{x})$ $(m = 1, \ldots, M)$, and weights are α_m $(m = 1, \ldots, M)$. Then the output of the final classifier is given by

$$H(\boldsymbol{x}) = \arg\max_k \sum_{m=1}^{M} \alpha_m \cdot \mathbb{I}\left(h_m(\boldsymbol{x}) = k\right), \qquad (1)$$

where $\mathbb{I}(\cdot)$ is the function that outputs 1 when the input is *true* and 0 when the input is *false*. The weak classifiers

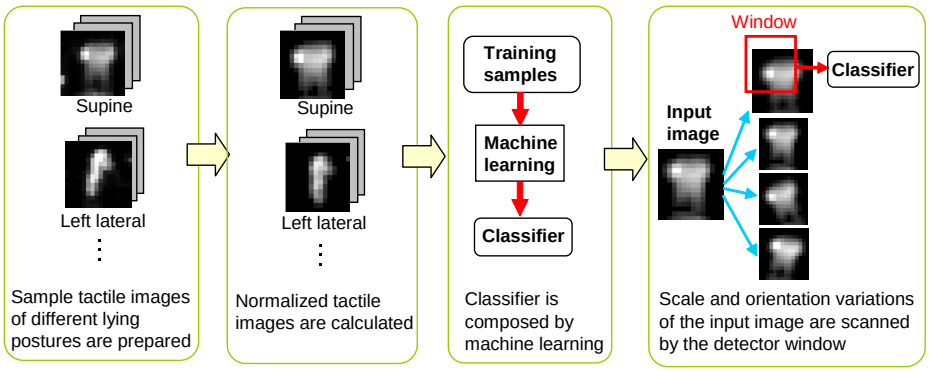

Figure 8. Basic processing flow for obtaining the location and posture of a person lying on a tactile sensor.

$h_m(\boldsymbol{x})$ and weights α_m in the final classifier are determined by learning. For output of the final classifier, we prepared five classes: supine, prone, right lateral, left lateral postures, and negative (not a lying posture).

Weak classifiers are defined so as to output one of the five classes above in response to the normalized tactile image as input. We adopt

$$h(\boldsymbol{x}) = \arg\min_k \rho_k \|\boldsymbol{x} - \boldsymbol{f}_k\|^2, \tag{2}$$

where $\boldsymbol{f}_k$ $(k = 1, \ldots, K)$ is a vector representing class k. A class whose $\boldsymbol{f}_k$ is the nearest to the input vector under weighting by ρ_k $(k = 1, \ldots, K)$ is selected as the output of the weak classifier, except in the following case. If, for a threshold $\theta > 1$,

$$\frac{l_2}{l_1} < \theta \tag{3}$$

where l_1 and l_2 are the first and second minimums of $\rho_k \|\boldsymbol{x} - \boldsymbol{f}_k\|^2$, then the output is the negative class, because no clear difference exists between the distances to the classes. Weak classifiers have parameters $\rho_k, \boldsymbol{f}_k, \theta$; by adopting different values for them, we can have different weak classifiers. Using SAMME, we select weak classifiers with specific parameters suitable for classification.

In the execution stage after learning, the input tactile images are larger than those in the learning stage and not normalized, so that we need to cope with variations in the location, orientation, size, and pressure range of the figure in the input image. For this purpose, our proposed method produces variations of the input image by scaling and rotating it, then our method scans the variations with a detection window connected to the classifier constructed by SAMME. The area of the scanned image overlapping with the detection window is cut out and vector-normalized, and then the result is sent to the classifier.

By scanning the image variations with the detection window, the best-matched location and posture are found and adopted as the output of the detection system. For this purpose, when one of four lying postures is output by the classifier connected to the detection window, not only the lying posture but also the confidence, defined as follows, is recorded for each detection window location.

$$[\text{Confidence}] = \max_k \sum_{m=1}^{M} \alpha_m \cdot \mathbb{I}\left(h_m(\boldsymbol{x}) = k\right) \tag{4}$$

Then the location and posture that have the maximum confidence are selected as the final output. By inversely applying scaling and rotation to the selected detection window, the location, size, and orientation of the figure in the original input image is obtained.

We employ the following parameters to specify the scanning method. The parameters are also determined according to the sample images.

Adjuster of the threshold in a weak classifier (θ_{adj}) When an input image is scanned, we substitute Eq. (3) with

$$\frac{l_2}{l_1} < \theta + \theta_{\mathrm{adj}},$$

where θ_{adj} is an adjusting value. In the execution stage, images larger than normalized images are input. An input image is scanned by the detection window and, as a result, images with a figure not standardized are also input to the classifier. To classify them to the negative class, we introduce θ_{adj}.

List of input image magnifications (L_{mag}) To absorb the size difference of the figure from the normalized images, a set of images with different magnifications is produced for scanning. L_{mag} is the list of the magnifications.

List of input image rotations (L_{rot}) To absorb the orientation difference of the figure from the normalized images, a set of images with different rotations is prepared for scanning. L_{rot} is the list of rotations.

Penalty for scale change (p_{mag}) Under the assumption that the figure size in the normalized image is the most common, the confidence in scale-changed image variations is reduced by multiplying

$$1 - p_{\mathrm{mag}} \times |1 - [\text{Magnification rate}]|.$$

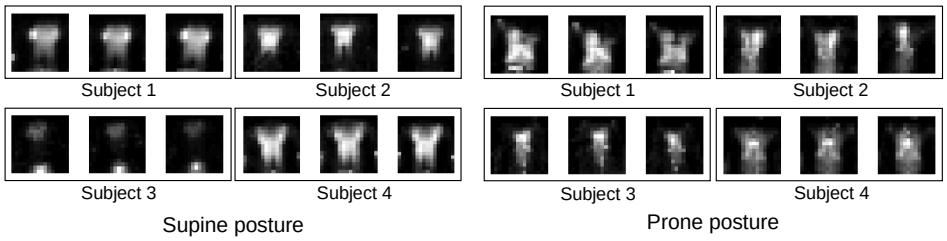

Figure 9. Examples of the original pressure patterns of the supine and prone postures.

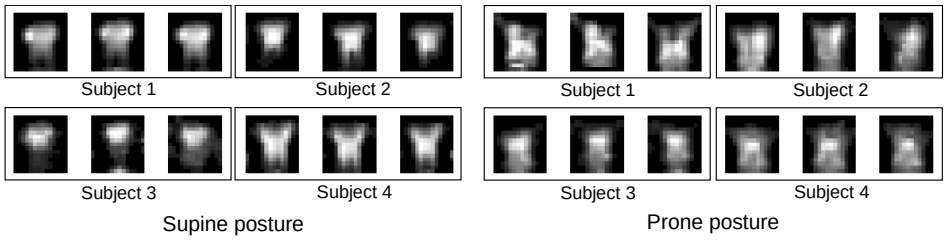

Figure 10. Examples of the normalized pressure patterns of the supine and prone postures.

Penalty for rotation (p_{rot}) Under the assumption that the figures in the normalized images have the most common orientation, the confidence in rotated image variations is reduced by multiplying

$$1 - p_{\mathrm{rot}} \times |1 - [\text{Rotation angle [rad]}]|.$$

The values of these parameters are determined by a thorough investigation of sample tactile images. The values that realize the smallest miss hit rate are selected from the candidates.

5 Evaluation

5.1 Samples Used

To evaluate the proposed method, we obtained tactile images when 11 persons were lying on the SR sensor in supine, prone, right lateral, and left lateral postures. We received written consent from the participants to the evaluation experiments . For each lying posture of each person, we obtained three tactile images because the lying location and posture change slightly in each trial. The attributes of the 11 subjects are shown in Table 1. As examples, the original tactile images obtained from four persons are shown in Figure 9. Pressure is indicated by a normalized grayscale image, in which white represents the maximum pressure and black represents no load. Images from the same posture of the same person have similar patterns, while those from different persons are somewhat different, even when they are in the same lying posture. Figure 10 shows normalized images of the original tactile images.

To evaluate the performance of the proposed method, we use leave-one-out cross validation. In this method, data from one person are extracted as test data, and the other data from 10 persons are used as training data. Then the miss hit rate is calculated for the test data. This procedure is repeated 11 times by changing the extracted person to obtain the average miss hit rate, which indicates the generalization error of the proposed method.

Table 1. Subject attributes.

	male	female
adult	6	3
child	1	1

5.2 Learning by SAMME

Classifiers of the lying postures were constructed by learning using SAMME. For candidates of the parameters of the weak classifiers, we used the following. For ρ_k, $\{1, 2, 3\}$ were prepared, and for θ, $\{1.05, 1.1, 1.2, 1.3\}$ were prepared. For the candidates of $\boldsymbol{f}_k$, we selected tactile images (converted to vectors) in posture k in the training data, one from each person. By combining all these candidates, the number of possible weak classifiers was $3^4 \times 4 \times 10^4 = 3,240,000$. From them, we selected $M = 30$ weak classifiers $h_m(\boldsymbol{x})$ and their weights α_m by using SAMME.

Figure 11 shows an example of the miss hit rates when SAMME was applied to data from a set of 10 persons. The other combinations of 10 persons had similar trends, where the miss hit rates were 0% for 10 or more weak classifiers. These low miss hit rates were obtained for normalized images, but the rate is expected to be higher for original input images. Thus, we obtained 30 weak classifiers to construct a final classifier.

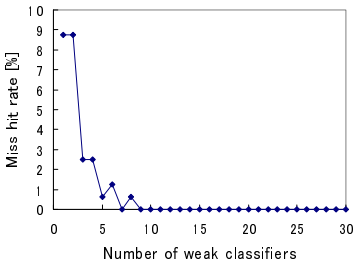

Figure 11. Miss hit rate in a learning procedure.

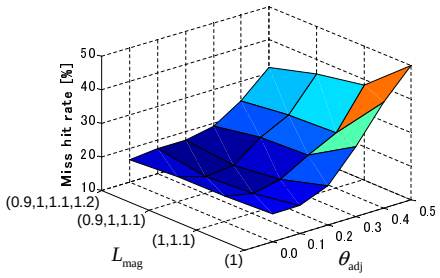

Figure 12. Searching the smallest miss hit rate by changing L_{mag} and θ_{adj}.

5.3 Search for Scan Parameters

For the scan parameters, we searched and selected the ones realizing the smallest miss hit rate for the training images. The candidates are as follows.

Adjuster of the threshold in a weak classifier (θ_{adj})
$\{0, 0.1, 0.2, 0.3, 0.4, 0.5\}$

List of input image magnifications (L_{mag})
$\{(1), (1, 1.1), (0.9, 1, 1.1), (0.9, 1, 1.1, 1.2)\}$

List of input image rotations (L_{rot})
$\{(0), (-0.26, 0, 0.26), (-0.52, -0.26, 0, 0.26, 0.52)\}$

Penalty for scale change (p_{mag}) $\{0, 1, 2\}$

Penalty for rotation (p_{rot}) $\{0, 1, 2\}$

For example, $L_{\mathrm{mag}} = (0.9, 1, 1.1)$ means that the input image is magnified by 0.9, 1, 1.1 to prepare three different-scale images for scanning. For the unit of rotation, the radian was adopted. Miss hit rates when L_{mag} and θ_{adj} were changed are shown in Figure 12. This procedure was conducted for all parameters.

After learning by SAMME for 30 weak classifiers, the scan parameters were determined. Miss hit rates in leave-one-out cross validation for the 11 sets of original training images without normalization and of test images are shown in Figure 13. Miss hit rates for normalized training images that were all 0% are not shown in this figure. The miss hit rates for test images 3 and 5 are higher than the others. This

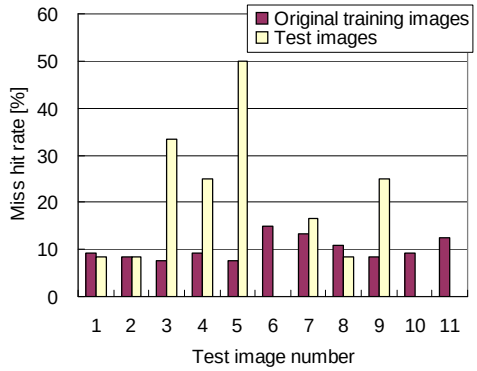

Figure 13. Miss hit rates of original training images and test images.

may be because these tactile images were largely different from the others because they were taken from children. The average miss hit rate is 10.1% for original training images, and 15.9% for test images.

5.4 Realtime Program

We developed a program that outputs in realtime the lying posture, the respiration rate, and the heart rate of the person on the SR sensor by using the learning results of SAMME for 30 weak classifiers and scan parameters. Four precision cells are set at pre-determined locations according to the classified lying posture. Three locations are selected for heartbeat detection and one for respiration detection, on the basis of the spectra of pressure from different cells, such as those shown in Figure 6, for each lying posture. We use one precision cell for respiration detection: if all precision cells are assigned to heartbeat detection, respiration oscillation that has different phases at each location may interfere and become small, though it is a rare occurrence. The FFT is applied to the average of four precision cell outputs containing respiration and heartbeat signals. Then, by finding the peaks in the corresponding bandwidths, the respiration rate and the heart rates are detected. For the FFT, 1024-point data during approximately 51 s are used. Samples of the average of the precision cell output, its FFT result, and detected frequencies for supine and prone postures are shown in Figure 14.

6 Conclusion

We have proposed a method for measuring the posture, respiration, and heartbeat of a person lying on a soft tactile sensor on a bed. To detect the heartbeat, precision measurements are needed and this takes some time. This limits the number of locations on the sensor where precision measurements are taken. In our method, a classifier of lying postures constructed by machine learning is used to de-

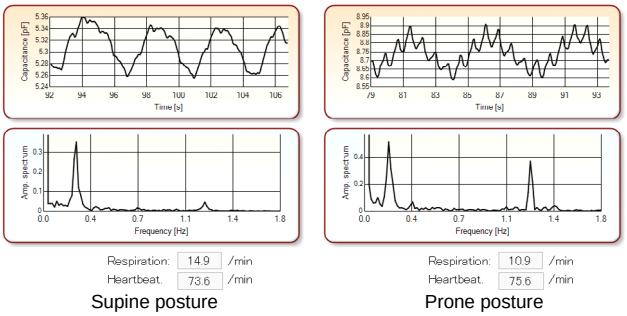

Figure 14. Average output of precision cells and its spectra from supine and prone postures.

termine these locations. We evaluated the system performance by using data sampled from 11 persons. The results showed that the average miss hit rate for new data is 15.9%. We developed a realtime measurement system based on this method.

In the current evaluation system, the tactile sensor is limited to the size of an upper body. If the size is larger and the hip and legs can be detected, it is expected that the miss hit rate of classification decreases. Extracting some feature values from pressure patterns before applying the classifier may also help reduce the miss hit rate. In future work, we will improve the accuracy of the lying posture classification and establish an unconstrained measurement system that does not disturb natural sleep. Our final goal is to develop a sleep monitoring system for deciding the quality of sleep and detecting diseases.

References

[1] S. Tanaka, Y. Matsumoto, and K. Wakimoto, Unconstrained and non-invasive measurement of heartbeat and respiration periods using a phonocardiographic sensor, *Medical and Biological Engineering and Computing*, *40*(2), 2002, 246-252.

[2] K. Watanabe, T. Watanabe, H. Watanabe, H. Ando, T. Ishikawa, and K. Kobayashi, Noninvasive measurement of heartbeat, respiration, snoring and body movements of a subject in bed via a pneumatic method, *IEEE Trans. on Biomedical Engineering*, *52*(12), 2005, 2100-2107.

[3] B.Y. Su, K.C. Ho, M. Skubic, and L. Rosales, Pulse rate estimation using hydraulic bed sensor, *Proc. 34th Annu. Int. Conf. of the IEEE EMBS (EMBC2012)*, San Diego, USA, 2012, 2587–2590.

[4] N. Bu, N. Ueno, and O. Fukuda, Monitoring of respiration and heartbeat during sleep using a flexible piezoelectric film sensor and empirical mode decomposition, *Proc. 29th Annu. Int. Conf. of the IEEE EMBS (EMBC2007)*, Lyon, France, 2007, 1362-1366.

[5] G.S. Chung, B.H. Choi, D.U. Jeong, and K.S. Park, Noninvasive heart rate variability analysis using loadcell-installed bed during sleep, *Proc. 29th Annu. Int. Conf. of the IEEE EMBS (EMBC2007)*, Lyon, France, 2007, 2357-2360.

[6] Y. Yamana, S. Tsukamoto, K. Mukai, H. Maki, H. Ogawa, and Y. Yonezawa, A sensor for monitoring pulse rate, respiration rhythm, and body movement in bed, *Proc. 33rd Annu. Int. Conf. of the IEEE EMBS (EMBC2011)*, Boston, USA, 2011, 5323-5326.

[7] C. Li, J. Lin, and Y. Xiao, Robust overnight monitoring of human vital signs by a non-contact respiration and heartbeat detector, *Proc. 28th Annu. Int. Conf. of the IEEE EMBS (EMBC2006)*, New York, USA, 2006, 2235-2238.

[8] Y. Nishida, M. Takeda, T. Mori, H. Mizoguchi, and T. Sato, Unrestrained and non-invasive monitoring of human's respiration and posture in sleep using pressure sensors, *J. of the Robotic Society of Japan*, *16*(5), 1998, 705-711 (in Japanese).

[9] S. Guo, Y. Kato, H. Ito and T. Mukai,Development of rubber-based flexible sensor sheet for care-related apparatus, *SEI Technical Review, 75*, 2012, 125-131.

[10] R. Cork, XSENSOR technology: a pressure imaging overview, *Sensor Review, 27*(1), 2007, 24-28.

[11] K. Matsuo, Y. Kato, A. Shimizu, S. Guo, and T. Mukai, Measurement of respiration and heartbeat using a flexible tactile sensor sheet on a bed, *Proc. 11th IASTED Int. Conf. on Biomedical Engineering (BioMed2014)*, Zurich, Switzerland, 2014 (Accepted).

[12] N. Cristianini and J. Shawe-Taylor, *An Introduction to support vector machines and other kernel-based learning methods* (Cambridge, UK; Cambridge University Press, 2000).

[13] Q. Le, M.A. Ranzato, R. Monga, M. Devin, J. Chen, G. Corrado, J. Dean, and A. Ng, Building high-level features using large scale unsupervised learning, *Proc. 29th Int. Conf. on Machine Learning (ICML2012)*, Edinburgh, Scotland, 2012, 81-88.

[14] L. Breiman, Random forests, *Machine Learning*, *45*(1), 2001, 5-32.

[15] Y. Freund and R. Schapire, A decision-theoretic generalization of on-line learning and an application to boosting, *Journal of Computer and System Science*, *55*, 1997, 119-139.

[16] J. Zhu, H. Zou, S. Rosset, and T. Hastie, Multi-class AdaBoost, *Statistics and its Interface*, *2*, 2009, 349-360.